COMMUNICATION

ChemComm
www.rsc.org/chemcomm

Chiral shape and enantioselective growth of colloidal particles of self-assembled meso-tetra(phenyl and 4-sulfonatophenyl)porphyrins†

Joaquim Crusats,[b] Josep Claret,[b] Ismael Díez-Pérez,[b] Zoubir El-Hachemi,[a] Héctor García-Ortega,[a] Raimon Rubires,[a] Francesc Sagués[b] and Josep M. Ribó*[a]

[a] *Department of Organic Chemistry, University of Barcelona, Martí i Franquès 1, 08028-Barcelona, Catalonia, Spain. E-mail: jmr@qo.ub.es*

[b] *Department of Physical Chemistry, University of Barcelona, Martí i Franquès 1, 08028-Barcelona, Catalonia, Spain*

Received (in Cambridge, UK) 26th March 2003, Accepted 13th May 2003
First published as an Advance Article on the web 29th May 2003

The self-assembly of diprotonated phenyl and 4-sulfonatophenyl meso-tetrasubstituted porphyrins gives a spontaneous chiral symmetry breaking, but only for $H_2TPPS_3^-$, which forms helicoidal colloidal particles; the selection of the resulting chirality sign by the hydrodynamic forces of a stirring vortex can be demonstrated.

The achiral water-soluble diprotonated porphyrins of Scheme 1 give, in acidic media, J-aggregates[1] which show spontaneous chiral symmetry-breaking.[2,3] In some cases the chirality sign (detected by circular dichroism spectroscopy†) could be selected by the direction of vortical stirring during formation of the homoassociates. The hydrodynamic forces, tiny as they might be, do not cause chiral symmetry breaking, but can select the sign of chirality at the symmetry bifurcation point.[4] Here we report on the chiral shape of the growing particles, which, together with their colloidal character, justify how the hydrodynamic forces can exert a detectable effect upon the enantioselective growth of homochiral particles.

Aggregates were obtained by rotary evaporation of dilute monomeric solutions.† The final solutions correspond to dilute gel solutions, in which the homoassociated porphyrins are the colloidal particles. For $H_2TPPS_3^-$ we obtain similar results to those previously published, *i.e*. the chirality sign was dependent on the direction of stirring and speed of the rotary evaporator. Stirring selection values of 80% at 300 rpm and 53% at 50 rpm [sets of 20 pairs of experiments (clockwise and anticlockwise)] were obtained. However, for the rest of the compounds of the H_2TPPS_x series stirring selection of the chirality sign could not be detected. This suggests a significant structural characteristic of the $H_2TPPS_3^-$ homoassociates.

All compounds of the H_2TPPS_x series show very similar absorption spectra,[2] which has been interpreted as a consequence of the exciton coupling perturbation limited to three neighbouring rings.[2,3] Therefore, structural differences arising from the different number of hydrophilic (4-sulfonatophenyl) or hydrophobic (phenyl) substituents and their relative substitution pattern must occur at a larger length scale than that originating from the electronic perturbation (> 40 Å).[2,5] This is confirmed by the different anisotropy values of their polarized fluorescence spectra in non-viscous media:[6] polarization (P) values of 0.4 for $H_2TPPS_4^{2-}$, similar to a previously reported determination ($P \approx 0.5$),[7] 0.13 for $H_2TPPS_3^-$ and H_2TPPS_{2o}, and 0.0 for H_2TPPS_{2a}. Being the anisotropy values related to the motion rates around the internal rotation axis (P = 0.5 for stick-like objects and 0 for spherical objects),[6] these results indicate considerable differences between the shapes of the aggregates of the series. An atomic force microscopy (AFM)†‡ study confirmed these results (*e.g*. see Figs. 1 and 2).

The homoassociate of each of these compounds show characteristic features, although their final shape and size also depends on whether or not they are obtained under stirring. In the case of $H_2TPPS_4^{2-}$ stick-like forms (Fig. 1a: 0.5–1.5 μm long, 40–50 nm wide and 5–15 nm high) were obtained without stirring. $H_2TPPS_4^{2-}$ homoassociates obtained from rotary evaporation of very dilute solutions exhibited the same type of structures, but a relatively large amount of irregular particles was detected and the sticks showed rounded ends (*e.g*. Fig. 1b and 1c). In the case of H_2TPPS_{2o} the particles correspond to stacked platelets, and for H_2TPPS_{2a} the homoassociates show round-shaped hemispherical-like particles, as those expected for the collapsing of spherical or oval colloidal particles after deposition on the mica substrate (Fig. 1). The most interesting result was obtained in $H_2TPPS_3^-$ aggregates (Fig. 2). For this compound we detect ribbons, showing homochiral folding coming from 3D helices, together with irregular potato-like

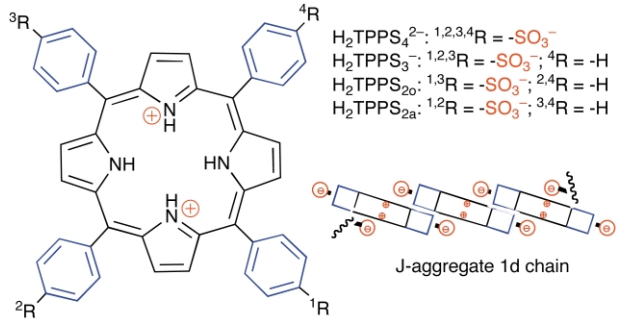

Scheme 1

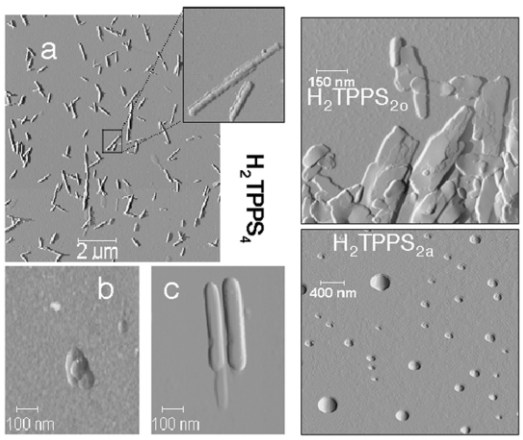

Fig. 1 AFM images (feedback amplitude signal) of aggregates coming from $H_2TPPS_4^{2-}$: (a) a concentrated solution (3.3 mM porphyrin, H_2SO_4, pH = 1.5) free of metallic cations [(10 × 10) μm². *Z* scale; 2 V. Inset (750 × 750) nm². *Z* scale; 0.1 V]; (b) and (c) rotary evaporated dilute solutions (final values: 4 μM porphyrin, 0.6 M NaCl, H_2SO_4, pH = 2.0) [(b) (700 × 700) nm². *Z* scale; 0.2 V. (c) (600 × 600) nm². *Z* scale; 0.2 V]. H_2TPPS_{2o} [(1 × 1) μm². *Z* scale; 0.2 V] and H_2TPPS_{2a} [(4 × 4) μm². *Z* scale; 0.3 V] coming from rotary evaporated dilute solutions (final values: 20 μM porphyrin, 0.6 M NaCl, H_2SO_4, pH = 1.5).

† Electronic supplementary information (ESI) available: procedures and methods. See http://www.rsc.org/suppdata/cc/b3/b303273f/

DOI: 10.1039/b303273f

particles and straight whiskers. Folded ribbons (1–3 μm length, 40–120 nm wide and a constant and uniform thickness of 3.2 ± 0.1 nm) were observed in stirred (rotary evaporation) and unstirred (sudden acidification of the free base porphyrin) samples but straight whiskers (0.7–1.5 μm length, 10–40 nm wide and a constant and uniform thickness of 2.3 ± 0.1 nm) were only observed in the case of unstirred solutions. The folding of the ribbons occurs between 50 and 120 nm, but noticeably exhibits a regular pitch when the width of the ribbon is constant. The pitch length decreases with the width, so that the widest ones show similar pitch and width lengths. In each sample, helices of both signs were always detected. Ribbons showing many foldings generally coil one-to-another forming bundles of helices of the same sign, which can also include the irregularly-shaped particles.†§

The different shapes of the homoassociates of the series H_2TPPS_x show the effect of the lateral hydrophobic phenyl groups on the packing between J-aggregate chains (Scheme 1). The significant result to stress here is that the chiral polarization exerted by the vortex direction could only be demonstrated for the compounds of the series giving helix-shaped aggregates ($H_2TPPS_3^-$), *i.e*. for colloidal particles with pronounced chiral shapes. For the following discussion of this result we take into account: a) the motion of a chiral shaped particle in a fluid, and b) the effect of a fluid motion on the electrical double layer of a colloidal particle.

The application of a uniform force to rigid enantiomeric chiral objects results in enantiomeric motions.[8–10] Furthermore, two enantiomers immersed in a fluid in chirotropic movement, *i.e*. the stirring vortex, will follow diastereotropic trajectories, or reciprocally, as recently shown, two enantiomeric micro objects with the same motion create diastereotropic fluid movements, which determine a different mass transport around each enantiomer.[11] As a consequence, it is conceivable to admit that the growth kinetics of the suspended chiral particles could be affected by stirring and that this would finally result in the enantioselective growth of hydrodynamically well-adapted mesoscopic shapes. This argument takes into account that the homochirality classification can be applied, *i.e*. two enantiomeric chiral shapes can be defined, such as occurs for helices but not in the case of the chiral potato shaped mesophases.[12] As a matter of fact, helices of different sign in a real fluid flow show strong differentiated motions.[13] In contrast, enantiomeric crystals of external chiral shape (*e.g*. the case of tartaric acid salts) show small differences between their mobility and resistance centres so that small differences between their motions must be expected. This should be kept in mind when comparing our observations here with the lack of experimental evidence of chiral sign selection by stirring in a crystallization context,[14] where only the initial stochastic symmetry breaking determines the chiral outcome. In the system herein studied (helix shaped "crystals") the enantioselective growth exerted by the hydrodynamic forces of the direction of stirring can overcome the initial excess of the less "adapted" enantiomer. The significance of the movement of chiral shaped macromolecules in complex systems was shown recently by the selection of right–left symmetry breaking in embryos by the direction of flow.[15]

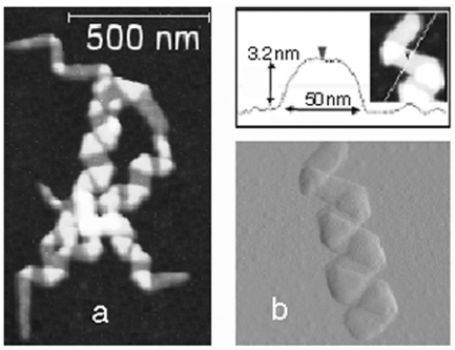

Fig. 2 AFM images of $H_2TPPS_3^-$ aggregates coming from solutions (3 μM porphyrin, 0.34 M NaCl, H_2SO_4 pH = 1.7) prepared by rotary evaporation. (a) Topography signal image of folded ribbons [(450 × 450) nm². *Z* scale; 0.1 V]. (b) Amplitude signal image of a helicoidal ribbon [(200 × 200) nm². *Z* scale; 0.1 V].

In the growth of colloidal particles (*e.g*. in a cluster-to-cluster mechanism) one principal contribution of the process activation energy is to overcome the repulsion originated by the diffuse electrical double layers.[16] It is noteworthy that the small dimension giving the colloidal character to the homoassociates of $H_2TPPS_3^-$ (ribbon thickness of 3.2 nm, see Fig. 2) is also where the growth occurs and chirality appears. Flow easily affects the diffuse electrical double layers,[8,9] by pushing the solution ions out. In consequence, the above described short range fluid movements could affect differentially the diffuse double layers of both enantiomeric objects, and result in higher enantioselection rates than expected for simple differential mass transport.

These results suggest that both the ionic or polar character of the supramolecular system and the pronounced structural asymmetry of the particulate mesophases are necessary conditions to select chirality by stirring vortices. In this respect, it is remarkable that both premises are found in peptides and nucleic acids, *i.e*. the result of primordial absolute asymmetric synthesis.

This study was supported by the MCYT of the Spanish Government (AGL2000-0975 and BXX2000-0638-102-01).

Notes and references

‡ The same shape was detected for the particles by AFM for different experimental conditions and substrates, but the best conditions were those obtained on mica substrates functionalized with amino propylsiloxane, according to similar procedures to those described for DNA samples.[17] The sample deposition procedure takes into account the colloidal nature of the solutions, and the anionic character of the homoassociate surface.

§ It was not possible to establish a correlation between the chirality sign (CD) of the sample with an excess of homochiral helices. In this respect, the small area character of the AFM measurements, the impossibility to scan completely the mica substrate, the groups of bundles of chiral shaped particles originated by the flocculation of gel drops.† prevent an statistical analysis of the homochirality of the deposited sample.

1 J. M. Ribo, J. Crusats, J.-A. Farrera and M. L. Valero, *J. Chem. Soc., Chem. Commun.*, 1994, 681–682.
2 R. Rubires, J.-A. Farrera and J. M. Ribo, *Chem. Eur. J.*, 2001, **7**, 436–446.
3 J. M. Ribo, J. Crusats, F. Sagues, J. M. Claret and R. Rubires, *Science*, 2001, **292**, 2063–2066.
4 D. K. Kondepudi and K. Asakura, *Acc. Chem. Res.*, 2001, **34**, 946–954.
5 M. Kasha, H. R. Rawls and M. A. El-Bayoumi, *Pure Appl. Chem.*, 1965, **11**, 371–392.
6 J. R. Lakowicz, *Principles of Fluorescence Spectroscopy*, 2nd edn., Kluwer Academic Publishers, New York, 1999, pp. 291–306.
7 O. Ohno, Y. Kaizu and H. Kobayashi, *J. Chem. Phys.*, 1993, **99**, 4128–4139.
8 S. Kim and S. J. Karrila, *Microhydrodynamics: Principles and Selected Applications*, Butterworth–Heinemann, Boston, 1991.
9 T. G. M. van de Ven, *Colloidal Hydrodynamics*, Academic Press, London, 1989.
10 P. G. de Gennes, *Europhys. Lett.*, 1999, **46**, 827–831.
11 B. A. Grzybowski and G. M. Whitesides, *Science*, 2002, **296**, 718–721.
12 E. Ruch, *Angew. Chem., Int. Ed. Engl.*, 1977, **16**, 65–72.
13 P. G. de Gennes, in *Symmetries and Broken Symmetries in Condensed Matter Physics*, ed. N. Boccara, Editions IDSET, Paris, 1981, pp. 1–9.
14 D. K. Kondepudi, R. J. Kaufman and N. Singh, *Science*, 1990, **250**, 975–977.
15 J. J. Essner, K. J. Vogan, M. K. Wagner, C. J. Tabin, H. J. Yost and M. Brueckner, *Nature*, 2002, **418**, 37–38.
16 J. O'M. Bockris, A. K. N. Reddy and M. Gamboa-Aldeco, in *Modern Electrochemistry*, **vol. 2A**, 2nd edn., Kluwer Academic Publishers, New York, 2000, pp. 1001–1006.
17 V. J. Morris, A. R. Kirby and A. P. Gunning, *Atomic Force Microscopy for Biologists*, Imperial College Press, London, 2000.